

Identification and analysis of residues contained on $\beta \rightarrow \alpha$ loops of the dual-substrate $(\beta\alpha)_8$ phosphoribosyl isomerase A specific for its phosphoribosyl anthranilate isomerase activity

Lianet Noda-García,¹ Aldo R. Camacho-Zarco,^{1,2} Karina Verdel-Aranda,^{1,2} Helena Wright,³ Xavier Soberón,² Vilmos Fülöp,^{3*} and Francisco Barona-Gómez^{1*}

¹Evolution of Metabolic Diversity Laboratory, Laboratorio Nacional de Genómica para la Biodiversidad (Langebio), CINVESTAV-IPN, Km 9.6 Libramiento Norte, Carretera Irapuato—León, Irapuato, C.P. 36822, México

²Departamento de Ingeniería Celular y Biotecnología, Instituto de Biotecnología, UNAM, Av. Universidad 2001, Cuernavaca, C.P. 62210, México

³Department of Biological Sciences, University of Warwick, Coventry CV4 7AL, United Kingdom

Received 5 November 2009; Revised 25 December 2009; Accepted 28 December 2009

DOI: 10.1002/pro.331

Published online 11 January 2010 proteinscience.org

Abstract: A good model to experimentally explore evolutionary hypothesis related to enzyme function is the ancient-like dual-substrate $(\beta\alpha)_8$ phosphoribosyl isomerase A (PriA), which takes part in both histidine and tryptophan biosynthesis in *Streptomyces coelicolor* and related organisms. In this study, we determined the Michaelis–Menten enzyme kinetics for both isomerase activities in wild-type PriA from *S. coelicolor* and in selected single-residue monofunctional mutants, identified after *Escherichia coli in vivo* complementation experiments. Structural and functional analyses of a hitherto unnoticed residue contained on the functionally important $\beta \rightarrow \alpha$ loop 5, namely, Arg¹³⁹, which was postulated on structural grounds to be important for the dual-substrate specificity of PriA, is presented for the first time. Indeed, enzyme kinetics analyses done on the mutant variants PriA_Ser⁸¹Thr and PriA_Arg¹³⁹Asn showed that these residues, which are contained on $\beta \rightarrow \alpha$ loops and in close proximity to the *N*-terminal phosphate-binding site, are essential solely for the phosphoribosyl anthranilate isomerase activity of PriA. Moreover, analysis of the X-ray crystallographic structure of PriA_Arg¹³⁹Asn elucidated at 1.95 Å herein strongly implicates the occurrence of conformational changes in this $\beta \rightarrow \alpha$ loop as a major structural feature related to the evolution of the dual-substrate specificity of PriA. It is suggested that PriA has evolved by tuning a fine energetic balance that allows the sufficient degree of structural flexibility needed for accommodating two topologically dissimilar substrates—within a bifunctional and thus highly constrained active site—without compromising its structural stability.

Keywords: $(\beta\alpha)_8$ -barrels; HisA and TrpF; phosphoribosyl isomerase A (PriA); dual-substrate specificity; loops motion; conformational diversity

Grant sponsor: Conacyt, Mexico; Grant numbers: 50952-Q, 83039; Grant sponsor: Joint international project of the Royal Society, United Kingdom.

*Correspondence to: Francisco Barona-Gómez, Evolution of Metabolic Diversity Laboratory, Laboratorio Nacional de Genómica para la Biodiversidad (Langebio), CINVESTAV-IPN, Km 9.6 Libramiento Norte, Carretera Irapuato—León, Irapuato, C.P. 36822, México. E-mail: fbarona@ira.cinvestav.mx or Vilmos Fülöp, Department of Biological Sciences, University of Warwick, Gibbet Hill Road, Coventry CV4 7AL, United Kingdom. E-mail: vilmos@globin.bio.warwick.ac.uk

Introduction

In recent years, enzyme promiscuity has “evolved” from being a biochemical curiosity to one of the main themes in the field of enzyme evolution,^{1,2} with a broad impact on the biotechnological applications of enzymes.^{3,4} The broad occurrence of enzyme promiscuity throughout all forms of cellular metabolism is well acknowledged,⁵ being more frequent in enzymes performing peripheral metabolic functions, such as those involved in the biosynthesis of natural products.^{6,7} Moreover, the feature of enzyme substrate promiscuity has been suggested to endow enzymes to be more evolvable,⁸ that is to reach a phenotypic trait with the smallest number of possible changes. However, despite the potential role of enzyme dual-substrate specificity on the evolution of enzyme functions, contemporary “generalist” enzymes that may serve as good experimental models to test evolutionary hypothesis are virtually nonexistent.

Such an enzyme model, which would allow experimental validation of evolutionary hypothesis, exists in the ancient-like dual-substrate ($\beta\alpha$)₈ phosphoribosyl isomerase A (PriA), which takes part in both histidine and tryptophan biosynthesis in *Streptomyces coelicolor* and *Mycobacterium tuberculosis*.⁹ This study showed that PriA has both *N*'-(5'-phosphoribosyl)anthranilate (PRA) isomerase (*trpF*, EC 5.3.1.24) and *N*'-[(5'-phosphoribosyl)formimino]-5-aminoimidazole-4-carboxamide ribonucleotide (ProFAR) isomerase (*hisA*, EC 5.3.1.16) activities, under physiologically relevant conditions. Remarkably, this generalist contemporary enzyme is capable of accommodating two quite structurally dissimilar substrates within a common active site (Fig. 1). Because PriA is closely related to HisA at the sequence and structural levels,^{10,11} understanding the molecular mechanisms that allowed acquisition of PRA isomerase activity in this ($\beta\alpha$)₈-barrel is a fundamental question with broad evolutionary implications for this protein fold.

From a structural perspective, there is evidence suggesting that PriA does exist in more than one “natural” conformation. Two independent wild-type structures of PriA of *S. coelicolor*, adopting different conformations, have been elucidated using X-ray crystallography, under virtually identical conditions, and at the same atomic resolution of 1.8 Å (PDBs: 1VZW¹⁰ and 2VEP¹¹). Furthermore, the two putative PriA conformers cooccur irrespective of the presence of substrates because these structures have bound sulphate ions, which can be taken as phosphate analogs present in the substrates. Thus, 1VZW has been suggested to adopt an open conformation, whereas 2VEP adopt a closed conformation. Interestingly, when these conformers are structurally superimposed, despite the fact that the root mean square deviation (RMSD) of the superimposed structures is

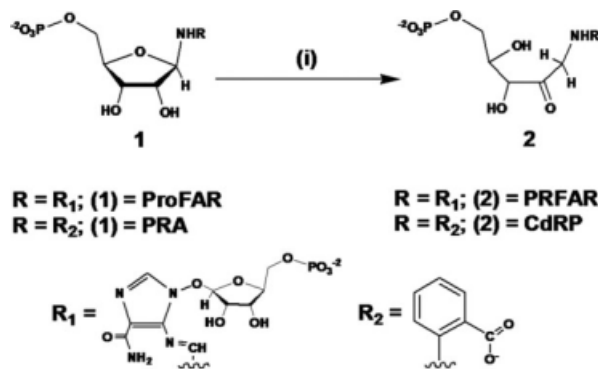


Figure 1. Enzymatic reactions of PriA, HisA, and TrpF.

(i) PriA, HisA, and TrpF catalyze Amadori rearrangements (isomerizations) on analogous phosphoribosyl substrates. PriA ($R = R_1$ or R_2), HisA ($R = R_1$), or TrpF ($R = R_2$). The products of ProFAR and PRA are *N*'-[(5'-phosphoribulose)formimino]-5-aminoimidazole-4-carboxamide ribonucleotide (PRFAR) and 1-[(2-carboxyphenyl)amino]-1-deoxyribulose 5-phosphate (CdRP), respectively.

only 0.32 Å (199 common C_α atoms), the distance between the last residues of the functionally important $\beta \rightarrow \alpha$ loops 1 and 6 that appear well defined in the open conformer of PriA, that is, Gly²³ (loop 1) and Ala¹⁶⁹ (loop 6), is of 4.83 Å and 4.11 Å, respectively.¹¹

In addition to the catalytic role of Asp¹¹ and Asp¹³⁰ common to the PRA and ProFAR isomerase activities of PriA, key molecular interactions with functional consequences, as probed by site-directed mutagenesis and *in vivo* complementation experiments using *Escherichia coli trpF* and *hisA* mutants, have been reported.¹¹ Among these, it was found that Ser⁸¹, which interacts with a sulphate ion at the *N*-terminal phosphate-binding site (PBS) through a molecule of water, and Arg¹⁹, which directly takes part in the C-terminal PBS, have important functional roles for the activities encoded by the *trpF* and *hisA* genes in *E. coli*, respectively. Moreover, a plausible molecular switch that may be mediating the different PriA conformers, involving an unusual C—H...O contact between Thr¹⁶⁶ and Asp¹⁷¹ was also identified. This interaction network is completed by a hydrogen bond between Asp¹⁷¹ and His²², which brings about loops 1 and 6, closing the active site. Mutation of any of these residues was found to affect *in vivo* the activities of PriA.¹¹

In this study, we determined the steady-state Michaelis–Menten enzyme kinetics for both PRA and ProFAR isomerase activities of wild-type PriA from *S. coelicolor* and the mutants PriA_{Arg}¹⁹Ala, PriA_{Ser}⁸¹Thr, and PriA_{Arg}¹³⁹Asn. Particular emphasis was put on the latter two mutants because mutation of Ser⁸¹ and Arg¹³⁹ was found to affect the PRA isomerase activity of this HisA-like enzyme. Moreover, the X-ray crystallographic structure of

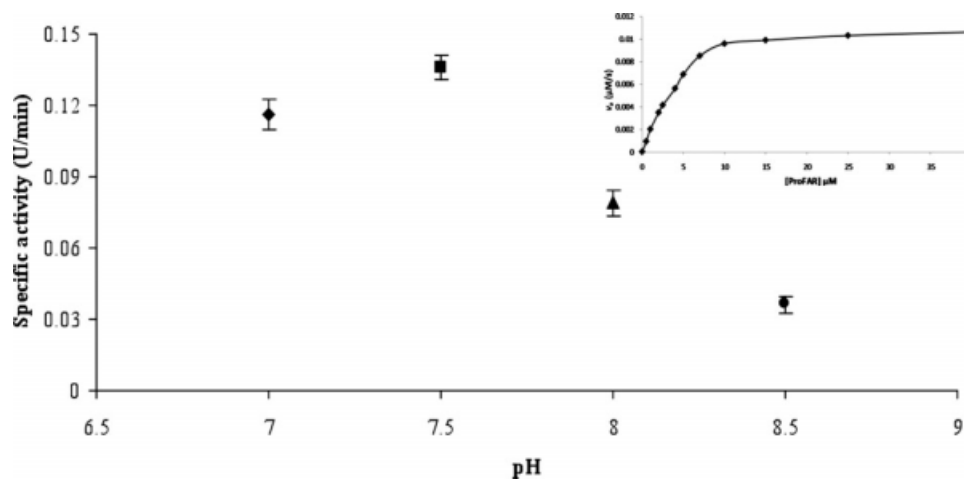


Figure 2. Specific ProFAR isomerase activity of PriA measured at different pHs. Specific ProFAR isomerase activity (at 25°C), defined as the moles of ProFAR that are catalyzed (at saturating concentrations, which equals 24 μM) per minute per milligram of purified PriA ($\text{U}/\text{min} = \mu\text{M mg}^{-1} \text{min}^{-1}$), was determined by triplicate. The Michaelis-Menten enzyme kinetic (v_o vs. $[S]$) shown in the inset (top-right corner) corresponds to ProFAR isomerase activity of PriA at a pH of 7.5, using an enzyme concentration of 25 nM.

PriA_Arg¹³⁹Asn elucidated at 1.95 Å was obtained, and this structure was used to explain the basis of the functional role of Arg¹³⁹. Based on these results, it was suggested that PriA has evolved its dual-substrate specificity by tuning a fine energetic balance, which allows the sufficient degree of structural flexibility needed for accommodating two topologically dissimilar substrates—within a bifunctional and thus highly constrained active site—without compromising its structural stability.

Results

Steady-state enzyme kinetics of PriA and selected mutants

Michaelis–Menten parameters were determined for the isomerization of the substrates PRA and ProFAR in wild-type PriA from *S. coelicolor*. The specific ProFAR isomerase activity of PriA was measured at different pHs, and the optimum pH was found to be 7.5 (Fig. 2). Because both isomerase activities of PriA are performed by the same set of catalytic residues

(Asp¹¹ and Asp¹³⁰), and thus, the mechanism of reaction can be assumed to be the same for both activities¹¹; the kinetic parameters using ProFAR and PRA as substrates were measured at this pH. Notably, our results disagree with the previously reported ProFAR isomerase kinetic parameters of PriA in at least one order of magnitude (Table I). This discrepancy was found to stem from the fact that the previously reported parameters were obtained at pH 8.5,¹⁰ which is one unit above the optimum pH experimentally determined herein. The differences found for the kinetic parameters using PRA as substrate (4-fold increase) may originate from a higher experimental standard error in the previous determination with regards to our data.

Previous results obtained by *in vivo* complementation of a *hisA* minus *E. coli* mutant showed that the mutant PriA_Arg¹⁹Ala lacks ProFAR isomerase activity.¹¹ This mutant was purified, and the steady-state enzyme kinetics analyses for both activities were performed. As expected, the level of PRA isomerase activity is similar to wild-type PriA; however,

Table I. Michaelis–Menten Kinetic Parameters of PriA and Selected Mutants

Enzyme ^a	ProFAR isomerase activity			PRA isomerase activity		
	K_M (μM)	k_{cat} (s^{-1})	k_{cat}/K_M ($\mu\text{M}^{-1} \text{s}^{-1}$)	K_M (μM)	k_{cat} (s^{-1})	k_{cat}/K_M ($\mu\text{M}^{-1} \text{s}^{-1}$)
PriA ^b	3.6 ± 0.7	1.3 ± 0.2	0.4	5 ± 0.08	3.4 ± 0.09	0.7
	28	0.9	0.03 ^b	4	12	3 ^b
PriA_Arg ¹⁹ Ala	4.1 ± 0.9	0.24 ± 0.5	0.06	8.3 ± 1.7	1.4 ± 0.2	0.2
PriA_Ser ⁸¹ Thr ^c	3.9 ± 0.8	0.33 ± 0.08	0.08	II ^d	II	0.0037 ^c
PriA_Arg ¹³⁹ Asn	3.6 ± 0.5	0.24 ± 0.01	0.07	II	II	II

^a Each datapoint is composed by at least three independent determinations using freshly purified enzyme, which was used to determine both activities simultaneously.

^b Data from the second row in PriA corresponds to the previously reported kinetic parameters for this enzyme.¹⁰

^c Despite the PRA isomerase activity of this mutant could be measured, its kinetic parameters could not be obtained (refer to text and Fig. 3).

^d II, immeasurably low.

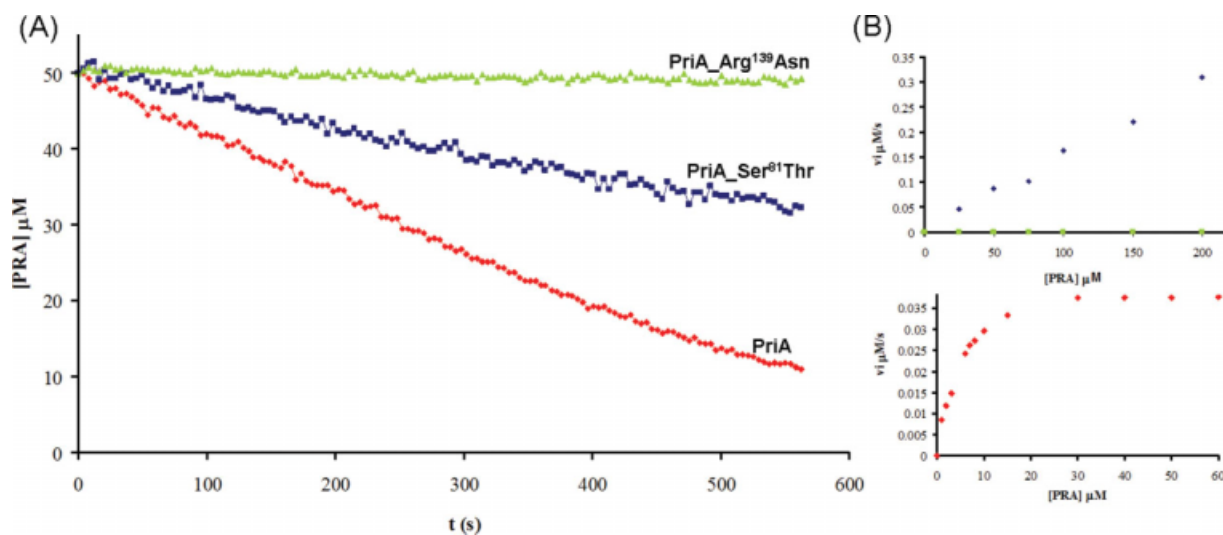


Figure 3. PRA isomerase activity of PriA and selected mutants. (A) Specific PRA isomerase activities of wild-type and selected mutants, using $1.5 \mu\text{M}$ of PriA_Arg¹³⁹Asn (green), $0.4 \mu\text{M}$ of PriA_Ser⁸¹Thr (blue), and $0.04 \mu\text{M}$ of PriA. (B) Michaelis-Menten enzyme kinetics (v_o vs. $[S]$) of PriA (red, lower panel) and selected mutants (upper panel), showing that PriA_Ser⁸¹Thr (blue) could not be saturated, and that PriA_Arg¹³⁹Asn (green) lacks all PRA isomerase activity. [Color figure can be viewed in the online issue, which is available at www.interscience.wiley.com.]

despite the fact that expression *in trans* of the mutant PriA_Arg¹⁹Ala fails to rescue the histidine auxotrophy of the *E. coli* *hisA* minus mutant Hfr G6¹¹, its catalytic ProFAR isomerase efficiency was found to be only five times less than wild-type PriA (Table I).

Based on similar *in vivo* complementation experiments, but using the *trpF* minus *E. coli* mutant FBG-W_f, the residue Ser⁸¹, which interacts through a molecule of water with the sulphate ion bound at the *N*-terminal PBS in the wild-type structure of PriA, was specifically implicated on its PRA isomerase activity.¹¹ In agreement with this, the mutant PriA_Ser⁸¹Thr was purified, and the determination of its steady-state enzyme kinetics showed that its ProFAR isomerase activity is similar to wild-type PriA, whilst its PRA isomerase catalytic efficiency is decreased by the mutation at least 200-fold. Given that the enzyme assay used for determining PRA isomerase activity follows disappearance of the substrate produced *in situ*, using more than $200 \mu\text{M}$ of anthranilic acid interferes with the fluorometric detection of PRA, rendering it impossible to saturate the enzyme. However, although the K_M and k_{cat} kinetic parameters for conversion of PRA could not be obtained, the catalytic efficiency was calculated from the lineal phase of the Michaelis–Menten equation [Fig. 3(B) and Table I].

In addition to residue Ser⁸¹, the sulphate ion bound at the *N*-terminal PBS of PriA interacts with residues Gly⁸³, Arg⁸⁵, Gly¹⁰⁴, Thr¹⁰⁵, and Arg¹³⁹. Interestingly, all these residues are located on the “hinges” of $\beta \rightarrow \alpha$ loops, which have been shown to be structurally and functionally important within the $(\beta\alpha)_8$ -barrel fold,¹² warranting further analysis

of these residues. Similarly to mutation of Ser⁸¹ into a Thr residue, it was hypothesized that by changing Arg¹³⁹ into a closely related Asn, the functional analysis of the original residue might be facilitated. A complete lack of PRA isomerase activity in this mutant was confirmed *in vivo* and *in vitro*, using enzyme saturation conditions (Fig. 3 and Table I). Interestingly, the ProFAR isomerase activity of this mutant was not significantly affected: the K_M of PriA_Arg¹³⁹Asn for the substrate ProFAR remained the same, whereas its k_{cat} is only five times smaller. Because both isomerase activities of PriA are accomplished by the same active site,¹¹ this result suggests that Arg¹³⁹ does not perform a catalytic role and that it is not related to binding of the substrate ProFAR.

Structural analysis of PRA isomerase minus PriA mutants

To understand the functional contribution of Ser⁸¹ and Arg¹³⁹ toward the PRA isomerase activity of PriA, crystallographic X-ray structural analyses of their corresponding mutants were pursued. Unfortunately, the mutant PriA_Ser⁸¹Thr could not be crystallized despite several attempts. In contrast, the structure of PriA_Arg¹³⁹Asn (PDB: 2x30), mutated at the functionally important $\beta \rightarrow \alpha$ loop 5, absent from 1VZW, could be resolved. This protein was purified and crystallized using similar conditions as for wild-type PriA.¹³ The structure of the PriA_Arg¹³⁹Asn mutant was obtained at a resolution of 1.95 \AA (Table II) and aligned with the structure of wild-type PriA, with a final RMSD of 0.24 \AA (213 common C α atoms). This allowed a comparison to be

Table 2. X-Ray Data Collection and Refinement Statistics

	PriA_Arg ¹³⁹ Asn (PDB: 2x30)
Data collection	
Synchrotron, detector and wavelength (Å)	ESRF BM16 ADSC Q210 CCD, 1.0074
Space group	P3 ₁ 21
Unit cell (<i>a</i> = <i>b</i> , <i>c</i> (Å))	63.6, 102.9
Resolution (Å)	28–1.95 (2.02–1.95)
Observations	182830
Unique reflections	18061
<i>I</i> / σ (<i>I</i>)	23.0 (2.4)
<i>R</i> _{sym} ^a	0.093 (0.652)
Completeness (%)	99.8 (100.0)
Refinement	
All nonhydrogen atoms	1846
Water molecules	126
Other solvent molecules	2 (sulfate)
<i>R</i> _{cryst} ^b	0.216 (0.359)
Reflections used	17365 (1269)
<i>R</i> _{free} ^c	0.273 (0.460)
Reflections used	696 (39)
<i>R</i> _{cryst} (all data) ^b	0.218
Mean temperature factor (Å ²)	39.2
RMSDS from ideal values	
Bonds (Å)	0.016
Angles (°)	1.4
DPI coordinate error (Å)	0.18

Numbers in parentheses refer to values in the highest resolution shell.

^a $R_{\text{sym}} = \sum_j \sum_h |I_{h,j} - \langle I_h \rangle| / \sum_j \sum_h \langle I_h \rangle$, where $I_{h,j}$ is the *j*th observation of reflection *h*, and $\langle I_h \rangle$ is the mean intensity of that reflection.

^b $R_{\text{cryst}} = \sum ||F_{\text{obs}}| - |F_{\text{calc}}|| / \sum |F_{\text{obs}}|$, where F_{obs} and F_{calc} are the observed and calculated structure factor amplitudes, respectively.

^c R_{free} is equivalent to R_{cryst} for a randomly selected subset of reflections not used in the refinement.

performed between wild-type PriA (PDB: 2VEP, chain A) and the mutant PriA_Arg¹³⁹Asn (Fig. 4) in terms of their temperature factors (B-factor), which are known to correlate with protein dynamics.

Although the structures of wild-type PriA and the mutant PriA_Arg¹³⁹Asn are overall quite similar, their loops 1, 5, and 6 were found to adopt significantly different conformations (Fig. 4). Loops 1 and 6 seem to be more flexible in PriA_Arg¹³⁹Asn than in wild-type structure, and a marked rigidity of loop 5 was only witnessed in the structure of the mutant. This observation was quantitatively supported by comparing the ratio of the B-factors of the residues contained on this loop over the whole structure. On average, the residues in loop 5 have 1.9 times higher B-factors than the corresponding values in the PriA_Arg¹³⁹Asn structure. This observation suggests that loop 5 of PriA is particularly flexible and that minor mutations can affect its dynamics, which in turn can have large functional consequences. Indeed, because this PriA mutant lacks its PRA isomerase activity, but not its ProFAR isomerase activity, it is tempting to speculate that Arg¹³⁹ is involved in mediating conformational changes, subsequently allowing the active site to adopt the right conformation to bind and/or turnover PRA productively.

Detailed analysis of the molecular environment of Arg¹³⁹ turned out to be informative in this respect. Despite the physicochemical differences between Asn and Arg, that is, the lack of a carbon atom and the presence of an amine (containing one N atom), instead of a guanidinium (containing three N atoms), these two residues are able to interact with the sulphate ion, fortuitously bound at the *N*-terminal PBS in both structures (Fig. 5). Interestingly, the residue taking position 139 in either structure adopts the same conformation, with their lateral chains pointing in the same direction toward the sulphate ion. However, when an Arg is located at position 139, two of the nitrogen atoms of the guanidinium group are able to form salt bridges with the sulphate ion, in contrast with only one contact that is found when Asn is taking this position.

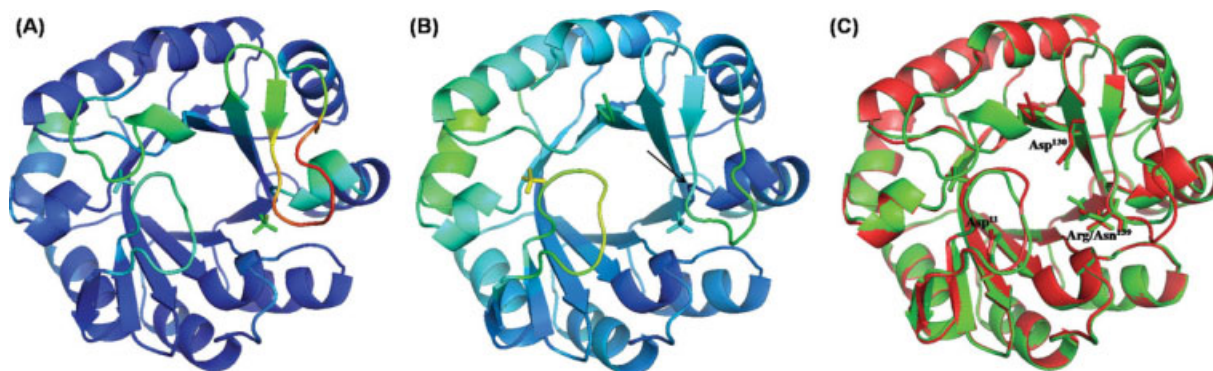


Figure 4. Structural differences between PriA and PriA_Arg¹³⁹Asn. (A) Wild-type PriA (PDB: 2VEP); and (B) PriA_Arg¹³⁹Asn mutant (this work, PDB: 2x30). The structures were colored from blue to red as the B-factors increase. Loop 5 is highlighted with a black arrow. (C) Structural superimposition of wild-type PriA (green) and PriA_Arg¹³⁹Asn (red). The sulphate ions bound to the two PBS, as well as residues Arg/Asn¹³⁹, Asp¹¹, and Asp¹³⁰, delimiting the boundaries of the active site, are also shown.

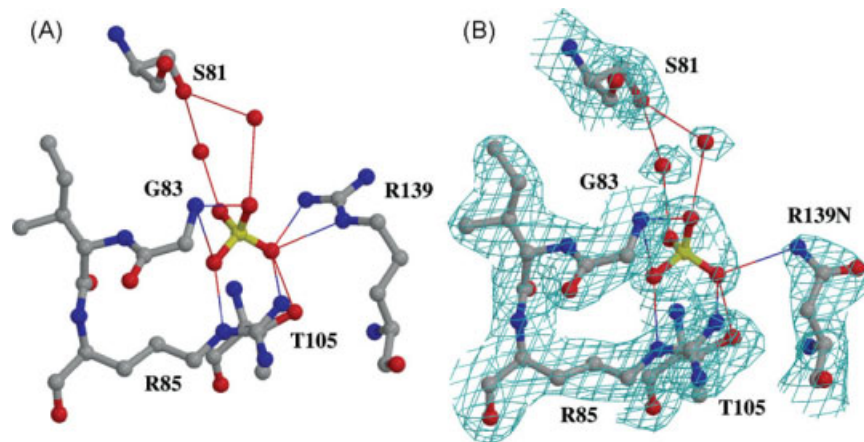


Figure 5. Molecular interactions of the residue adopting position 139. (A) Interactions of Arg in wild-type PriA; the electron density of this structure has been reported previously¹¹; and (B) Interactions of Asn in PriA_Arg¹³⁹Asn. Hydrogen bonds are drawn as thin lines. The SIGMAA¹⁴ weighted 2mFo-ΔFc electron density using phases from the final model is contoured at 1σ level, where σ represents the root mean square deviation electron density for the unit cell. Contours more than 1.4 Å from any of the displayed atoms, other than Ser⁸¹, have been removed for clarity. Figure was drawn using Molscrip^{15,16} and rendered with Raster 3D.¹⁷ [Color figure can be viewed in the online issue, which is available at www.interscience.wiley.com.]

This is the only change observed in the binding of the *N*-terminal sulphate ion when PriA and PriA_Arg¹³⁹Asn are compared.

Discussion

Previous characterization of HisA enzymes from *Thermotoga maritima* and *E. coli*, including single-residue mutants, implied a correlation between results obtained *in vivo* and *in vitro*.¹⁸ Based on these observations, an *in vivo* genetic screening for identifying key residues involved in the evolution of the dual-substrate specificity of PriA was adopted. Indeed, previous *in vivo* results implicated residues Arg¹⁹ and Ser⁸¹ in the specific conversions of ProFAR and PRA, respectively.¹¹ Although this approach has simplified the analysis of a large collection of mutants, the fact that the enzyme kinetic parameters obtained for PriA_Arg¹⁹Ala does not agree with the inability of this mutant to complement a *hisA* mutation may raise some doubts about the validity of this approach. False negatives due to technical problems can be ruled out because many mutants were simultaneously analyzed, rendering reproducible results. An alternative explanation to this discrepancy may have to do with the recent appreciation that functional performance of enzymes *in vivo* is not limited to catalytic proficiency, as measured *in vitro*.¹⁹ Such “*in vivo* characteristics,” necessarily encoded by the enzyme’s primary sequence, may relate to protein stability, protein expression, and protein-protein interactions, amongst other unknown context-dependent factors. Irrespective of the nature of this discrepancy, the difficulty in identifying residues specifically related to the ProFAR isomerase activity may be taken as a reflection of the ancestral origin of this activity in PriA, which is conserved in all HisA bacterial homologs.

In the cases where the enzyme assays confirmed that the inability to complement a *trpF* mutation was related to a lack of PRA isomerase activity, that is, PriA_Ser⁸¹Thr and PriA_Arg¹³⁹Asn, it was particularly encouraging to find that these mutations do not affect the mechanism of reaction, as suggested by the fact that ProFAR could still be converted quite efficiently. Indeed, functional analysis of these ProFAR isomerase monofunctional PriA mutants does bring about novel insights into the evolution of the PRA isomerase activity in this HisA-like (βα)₈-barrel. An interesting observation is that their *K*_M and *k*_{cat} kinetic parameters for conversion of ProFAR imply that these residues, which were presumed to be part of the *N*-terminal PBS as suggested by their closeness with the sulphate ion, must be unrelated to the binding of the phosphate moieties of the substrates. Moreover, because it is safe to assume that these residues do not perform a catalytic role, and that ProFAR and PRA most likely are bound by their common phosphate moieties, the question of how these mutations have abolished the ability to convert PRA is a complex one, as discussed later.

The kinetic parameters obtained for the ProFAR isomerase activity are consistent with two possibilities: (i) that mutation of Ser⁸¹ and Arg¹³⁹, which are contained on β → α flexible loops, may have affected the ability of PriA to adopt the natural conformation of the active site, compromising completely turnover of PRA, as well as that of ProFAR 5-fold; and (ii) that PriA uses residues Ser⁸¹ and Arg¹³⁹ for binding of PRA, but not of ProFAR, as suggested by the unaffected *K*_M parameter obtained for the latter substrate. Furthermore, although the *k*_{cat} and *K*_M kinetic parameters for PriA_Ser⁸¹Thr, with regards to PRA, could not be obtained, our

ability to detect PRA isomerase activity *in vitro* is consistent with the idea that this residue is not involved in a discreet catalytic step or binding of the phosphate moiety. Given that PRA and ProFAR have in common a phosphoribosyl moiety, by which these substrates must be primarily bound by PriA, but that they differ in their aromatic anomeric group, it could be that these residues are specifically involved in recognition of the anthranilate moiety of PRA, with a concomitant negative effect on the turnover of this substrate. This would also suggest that the C-terminal PBS, as opposed to our previous proposal based solely in *in vivo* complementation assays, does not bind PRA.¹¹ Interestingly, multisequence alignments of HisA and PriA enzymes suggest so far that Ser⁸¹ and Arg¹³⁹ are specific to PriA (F. B. -G. and L. N. -G., unpublished observations).

The structural analysis of PriA_Arg¹³⁹Asn is in agreement with the conclusion that Ser⁸¹ and Arg¹³⁹ are involved in the specific recognition, and subsequent turnover, of PRA. In accordance with Jensen's hypothesis on the evolution of metabolic pathways through enzyme recruitment,²⁰ the most likely solution for the evolution of the PRA isomerase activity in the scaffold of PriA would imply the acquisition of changes related to the binding capabilities. However, because both PRA and ProFAR have analogous phosphates, subtle changes not related to the PBS would have to occur. As demonstrated by the structural analysis, the N-terminal PBS of wild-type PriA and PriA_Arg¹³⁹Asn are identical. In contrast, loss of PRA isomerase activity in PriA_Arg¹³⁹Asn is concomitant with an increased rigidity of the $\beta \rightarrow \alpha$ loop 5. In agreement with this, Ser⁸¹ is located relatively far from the sulphate ion, but within the functionally important $\beta \rightarrow \alpha$ loop 3. These observations suggest that modification of the dynamics of $\beta \rightarrow \alpha$ loops, which are generally accepted to be important for this protein fold,^{12,21} may have a major role on the evolution of the dual-substrate specificity of PriA. In agreement with this, loops have been implicated in the gain-and-loss of enzymatic activities in other protein folds.^{22,23}

The proposed protein conformational diversity of PriA, which implies cooccurrence of different conformers of the same protein in solution—independent of an induced fit mechanism—could be related to the evolution of the dual substrate specificity of PriA. A link between the evolution of novel enzyme functions, starting from a promiscuous enzyme activity as an evolutionary raw material, and protein conformational diversity, has been previously postulated.^{24,25} This proposal stems from studies on antibodies, where it has been shown that these can indeed exist as a mixture of conformers, capable of promiscuously binding “unnatural” antigens.²⁴ The appearance of PriA from a HisA-like monofunctional promiscuous enzyme might be seen as an interesting example of this possi-

bility, and thus further investigation of the motion of the active site loops of this ($\beta\alpha$)₈-isomerase, by means of X-ray crystallography of complexes between enzyme and transition-state analogues or noncrystallographic methods compatible with analysis in solution,²¹ are very promising. The hypothesis along these lines would be that PriA has evolved its PRA isomerase activity by tuning a fine energetic balance that allows the sufficient degree of structural flexibility needed for accommodating two topologically dissimilar substrates—within a bifunctional and thus highly constrained active site – without compromising its structural stability.

Materials and Methods

Site-directed mutagenesis

The mutant PriA_Arg¹³⁹Asn was constructed using the megaprimer method²⁶ using as template the plasmid pGEX-PriA-*Sco*.⁹ The sequences of the mutagenic oligonucleotides were as follows: R139For, 5'/ccgcggc aat ggctggaccgcgacggcgcg and R139Rev, 5'/cgcgccgtcggggtccagcc att gccgcg. All constructs were sequenced before functional analyses.

Biochemical characterization of PriA and its mutants

In vivo complementation of *hisA* and *trpF* minus *E. coli* mutants was performed as described previously.¹¹ Expression and purification of wild-type PriA and its mutants was performed from the expression vector pET-15b (Stratagene) as described previously.¹³ Michaelis-Menten enzyme kinetics of ProFAR and PRA isomerase activities were determined using reported protocols^{14,27} with minor modifications, as discussed later. The kinetic parameters were obtained fitting initial rates to the Michaelis-Menten model using nonlinear fit analysis with the publicly available program MicroCal Origin 5.0. Each datapoint included in Table I represents at least three independent experiments using freshly purified enzyme, which was simultaneously assayed for both activities.

ProFAR was synthesized, purified, and quantified according to the method described previously,²⁸ using phisGIE-tac and pBS111R plasmids, kindly provided by V. Jo Davisson and Rebecca S. Myers. The HisF subunit of the imidazol glycerol phosphate synthase from *T. maritima* (*thisF*) was subcloned from plasmid pET11c-*thisF*, kindly provided by Prof. Reinhard Sterner and coworkers,²⁹ into the plasmid pET-15b (Novagen) by using the restriction sites *NdeI* and *BamHI*. Plasmid pET15b-*thisF* was used to purify this enzyme by Nickel affinity columns HisTrap HP (GE Healthcare) attached to an Äkta FPLC from Amersham Biosciences. ProFAR isomerase reactions were performed at 25°C and followed spectrophotometrically at 300 nm, in the presence of

50 mM TES-HCl buffer (pH 7.5), 200 mM of ammonium acetate, in a Varian Cary 100 BIO UV-visible spectrophotometer. An excess of purified tHisF (2 μ M final concentration) was added to the reaction mix to avoid product inhibition.¹⁸

For the PRA isomerase enzyme assay, the gene encoding for indol 3-glycerol phosphate synthase from *T. maritima* (tIGPS) was subcloned from plasmid pET tmtrpC 21a³⁰ (kindly provided by R. Sterner) into a modified version of pQE30 (Qiagen), termed pQEI (F.B.-G. and L.N.-G., unpublished results), using the restriction sites *Nde*I and *Hind*III to generate plasmid pQEItmIGPS. Anthranilate phosphoribosyl transferase from *Saccharomyces cerevisiae* (γ AnPRT) expressed from plasmid pET γ AnPRT 28a (also provided by R. Sterner), and tIGPS expressed from pQEItmIGPS, were purified by Nickel affinity using the same Nickel affinity—FPLC system. Initial rates for PRA isomerase activity were measured at 25°C using enzymatically produced PRA in 50 mM Tris-HCl (pH 7.5), 4 mM MgCl₂, 4 mM EDTA, 0.4 μ M DTT, 0–200 μ M anthranilic acid (Sigma), a 5-fold molar excess of PRPP (Sigma), and 1 μ M of γ AnPRT. Both reactions (PRA production and its subsequent conversion) were followed fluorometrically in 96-well plates (Nuc 96 Well Optical Bottom Plates) in a TECAN infinite M1000 plate reader (excitation at 310 nm and emission at 400 nm). tIGPS was added to avoid product inhibition.

Crystallization, X-ray data collection, structure determination, and refinement

The PriA_{Arg}¹³⁹Asn mutant was expressed and purified as reported previously for wild-type PriA. Crystals were obtained after 48 hr of incubation in the same condition as reported previously.¹³ X-ray data were processed using the HKL suite of programs.³¹ Refinement of the structure was carried out using the coordinates of 2VEP by alternate cycles of REFMAC³² and manual refitting using O.³³ Water molecules were added to the atomic model automatically using ARP³⁴ at the positions of large positive peaks in the difference electron density, only at places where the resulting water molecule fell into an appropriate hydrogen bonding environment. Restrained isotropic temperature factor refinements were carried out for each individual atom. Data collection and refinement statistics are given in Table II.

Acknowledgments

We are indebted to Nobuhiko Tokuriki for useful discussions and critical reading of the manuscript, and to the reviewers for their useful suggestions to improve this manuscript. We thank V. Jo Davisson, Rebecca S. Myers, and Reinhard Sterner for providing plasmids and strains. Crystallographic data were collected at

beamline BM16 at the ESRF, France, and we acknowledge the support of Ana Labrador.

References

1. Mannervik B, Runarsdottir A, Kurtovic S (2009) Multi-substrate-activity space and quasi-species in enzyme evolution: Ohno's dilemma, promiscuity and functional orthogonality. *Biochem Soc Trans* 37:740–744.
2. Tracewell CA, Arnold FH (2009) Directed enzyme evolution: climbing fitness peaks one amino acid at a time. *Curr Opin Chem Biol* 13:3–9.
3. Hult K, Berglund P (2007) Enzyme promiscuity: mechanism and applications. *Trends Biotechnol* 25:231–238.
4. Nobeli I, Favia AD, Thornton JM (2009) Protein promiscuity and its implications for biotechnology. *Nat Biotechnol* 27:157–167.
5. Khersonsky O, Roodveldt C, Tawfik DS (2006) Enzyme promiscuity: evolutionary and mechanistic aspects. *Curr Opin Chem Biol* 10:498–508.
6. O'Maille PE, Malone A, Dellas N, Andes Hess B, Jr, Smentek L, Sheehan I, Greenhagen BT, Chappell J, Manning G, Noel JP (2008) Quantitative exploration of the catalytic landscape separating divergent plant sesquiterpene synthases. *Nat Chem Biol* 4:617–623.
7. Des Marais DL, Rausher MD (2008) Escape from adaptive conflict after duplication in an anthocyanin pathway gene. *Nature* 454:762–765.
8. Aharoni A, Gaidukov L, Khersonsky O, Mc QGS, Roodveldt C, Tawfik DS (2005) The 'evolvability' of promiscuous protein functions. *Nat Genet* 37:73–76.
9. Barona-Gomez F, Hodgson DA (2003) Occurrence of a putative ancient-like isomerase involved in histidine and tryptophan biosynthesis. *EMBO Rep* 4:296–300.
10. Kuper J, Doenges C, Wilmanns M (2005) Two-fold repeated (beta/alpha)₄ half-barrels may provide a molecular tool for dual substrate specificity. *EMBO Rep* 6:134–139.
11. Wright H, Noda-Garcia L, Ochoa-Leyva A, Hodgson DA, Fulop V, Barona-Gomez F (2008) The structure/function relationship of a dual-substrate (beta/alpha)₈-isomerase. *Biochem Biophys Res Commun* 365:16–21.
12. Ochoa-Leyva A, Soberon X, Sanchez F, Arguello M, Montero-Moran G, Saab-Rincon G (2009) Protein design through systematic catalytic loop exchange in the (beta/alpha)₈ fold. *J Mol Biol* 387:949–964.
13. Wright H, Barona-Gomez F, Hodgson DA, Fulop V (2004) Expression, purification and preliminary crystallographic analysis of phosphoribosyl isomerase (PriA) from *Streptomyces coelicolor*. *Acta Cryst D* 60:534–536.
14. Read RJ (1986) Improved Fourier coefficients for maps using phases from partial structures with errors. *Acta Cryst A* 42:140–149.
15. Kraulis PJ (1991) Molscript—a program to produce both detailed and schematic plots of protein structures. *J Appl Cryst* 24:946–950.
16. Esnouf RM (1997) An extensively modified version of MolScript that includes greatly enhanced coloring capabilities. *J Mol Graphics Model* 15:132.
17. Merritt EA, Murphy MEP (1994) Raster3d Version 2.0—a program for photorealistic molecular graphics. *Acta Cryst D* 50:869–873.
18. Henn-Sax M, Thoma R, Schmidt S, Hennig M, Kirschner K, Sterner R (2002) Two (beta/alpha)₈-barrel enzymes of histidine and tryptophan biosynthesis have similar reaction mechanisms and common strategies for protecting their labile substrates. *Biochemistry* 41:12032–12042.

19. Yoshikuni Y, Dietrich JA, Nowroozi FF, Babbitt PC, Keasling JD (2008) Redesigning enzymes based on adaptive evolution for optimal function in synthetic metabolic pathways. *Chem Biol* 15:607–618.
20. Jensen RA (1976) Enzyme recruitment in evolution of new function. *Annu Rev Microbiol* 30:409–425.
21. Wang Y, Berlow RB, Loria JP (2009) Role of loop-loop interactions in coordinating motions and enzymatic function in triosephosphate isomerase. *Biochemistry* 48:4548–4556.
22. Park HS, Nam SH, Lee JK, Yoon CN, Mannervik B, Benkovic SJ, Kim HS (2006) Design and evolution of new catalytic activity with an existing protein scaffold. *Science* 311:535–538.
23. Doucet N, Watt ED, Loria JP (2009) The flexibility of a distant loop modulates active site motion and product release in ribonuclease A. *Biochemistry* 48:7160–7168.
24. James LC, Tawfik DS (2003) Conformational diversity and protein evolution—a 60-year-old hypothesis revisited. *Trends Biochem Sci* 28:361–368.
25. Tokuriki N, Tawfik DS (2009) Protein dynamism and evolvability. *Science* 324:203–207.
26. Xu Z, Colosimo A, Gruenert DC (2003) Site-directed mutagenesis using the megaprimer method. *Methods Mol Biol* 235:203–207.
27. Hommel U, Eberhard M, Kirschner K (1995) Phosphoribosyl anthranilate isomerase catalyzes a reversible amadori reaction. *Biochemistry* 34:5429–5439.
28. Davisson VJ, Deras IL, Hamilton SE, Moore LL (1994) A plasmid-based approach for the synthesis of a histidine biosynthetic intermediate. *J Org Chem* 59:137–143.
29. Thoma R, Obmolova G, Lang DA, Schwander M, Jenö P, Sterner R, Wilmanns M (1999) Efficient expression, purification and crystallisation of two hyperthermostable enzymes of histidine biosynthesis. *FEBS Lett* 454:1–6.
30. Merz A, Knochel T, Jansonius JN, Kirschner K (1999) The hyperthermostable indoleglycerol phosphate synthase from *Thermotoga maritima* is destabilized by mutational disruption of two solvent-exposed salt bridges. *J Mol Biol* 288:753–763.
31. Otwinowski Z, Minor W (1997) Processing of X-ray diffraction data collected in oscillation mode. *Macromol Cryst A* 276:307–326.
32. Murshudov GN, Vagin AA, Dodson EJ (1997) Refinement of macromolecular structures by the maximum-likelihood method. *Acta Cryst D* 53:240–255.
33. Jones TA, Zou JY, Cowan SW, Kjeldgaard M (1991) Improved methods for building protein models in electron-density maps and the location of errors in these models. *Acta Cryst A* 47:110–119.
34. Perrakis A, Sixma TK, Wilson KS, Lamzin VS (1997) wARP: Improvement and extension of crystallographic phases by weighted averaging of multiple-refined dummy atomic models. *Acta Cryst D* 53:448–455.